Frequency-Domain Equalization for MIMO-OFDM over Doubly Selective Channels

Mojtaba Beheshti, Mohammad Javad Omidi and Ali Mohammad Doost-Hoseini
Department of Electrical and Computer Engineering
Isfahan University of Technology
Isfahan, Iran 84156-83111
Email: m.beheshti@ec.iut.ac.ir, {omidi, alimdh}@cc.iut.ac.ir,

***Abstract*— Orthogonal frequency division multiplexing (OFDM) systems may confront significant intercarrier interference (ICI) when applied in doubly selective channels. Furthermore, the insufficient cyclic prefix (CP) leads to interblock interference (IBI) which again results in ICI. These interferences cause an early error floor in conventional receivers. In this paper, we characterize the doubly selective channel using a basis expansion model (BEM) and propose a frequency-domain equalization approach to jointly combat the ICI and IBI. We also derive a low-complexity scheme for the proposed approach. Simulation results show the superior performance of the proposed equalizer.**

Keywords- MIMO, OFDM, doubly selective channel, intercarrier interference (ICI), interblock interference (IBI), equalization.

I. Introduction

The combination of multiple-input multiple-output (MIMO) technology and orthogonal frequency division multiplexing (OFDM) is considered as a viable solution for future wireless communication systems [1], [2]. MIMO techniques provide diversity, multiplexing, or antenna gain, thereby improve the error performance, the bit rate, or the signal-to-interference-plus-noise ratio (SINR), respectively. On the other hand, OFDM modulation combats frequency selective fading effectively by dividing a wideband frequency selective fading channel into parallel narrowband flat fading subchannels. OFDM systems could maintain the orthogonality among subcarriers if the channel response is not changed during the OFDM block. But next generation wireless applications are expected to operate at high carrier-frequencies, at high capacities, and at high levels of mobility, resulting time- and frequency-selective, or doubly selective fading. In this case, intercarrier interference (ICI) occurs due to the loss of orthogonality. Moreover, interblock interference (IBI) arises when the channel delay span is larger than the cyclic prefix (CP), which again results in ICI. Hence, equalization techniques are required to restore the orthogonality and so to eliminate ICI/IBI.

There are many attempts in the literature for interference cancellation and equalization of MIMO-OFDM systems. Authors in [3], have designed ICI-mitigating block linear filters based on SINR maximization. In [4], the received frequency-domain signals are divided into subbands and then, joint soft ICI cancellation and decoding is performed. Ref. [5] applies a channel estimation method and uses the estimated parameters to reproduce the interference components, which are then iteratively cancelled from the received signal. A MIMO-OFDM system without CP is considered in [6] and a two-step interference cancellation and signal detection algorithm is proposed. The algorithm is based on some structural properties derived from shifting the received OFDM blocks. To solve the mobility-induced ICI problem, a low-complexity zero-forcing (ZF) approach is presented in [7]. The main idea is to explore the special structure inherent in the ICI matrix and apply Newton's iteration method for matrix inversion. However, most of the existing literature, including the above-mentioned works, do not consider a fast time-varying (TV) channel in conjunction with an insufficient CP.

In this paper, we consider a general case where the channel varies within each OFDM block and the CP length is shorter than the delay span of the channel. We propose a per-tone frequency-domain equalizer to jointly mitigate the ICI and IBI for MIMO-OFDM transmission system. The rest of this paper is organized as follows. In Section II, we describe the system, channel, and data models. We introduce the proposed equalizer in Section III. We derive a low-complexity scheme for the proposed equalizer in Section IV. In Section V, we show that our framework unifies and extends many previously proposed equalization methods. In Section VI, we present the simulation results. Finally, we conclude the paper in Section VII.

Notation: We use upper (lower) case bold-face letters to denote matrices (column vectors). Superscripts $(\cdot)^T$ and $(\cdot)^H$ represent transpose and Hermitian, respectively. $\mathcal{E}\{\cdot\}$ stands for the expectation, $\otimes$ represents the Kronecker product and diag$\{\mathbf{x}\}$ indicates a diagonal matrix with $\mathbf{x}$ as diagonal. We use x_n to indicate the nth element of vector $\mathbf{x}$. We denote the $m \times p$ all-zero matrix by $\mathbf{O}_{m\times p}$. $\boldsymbol{\mathcal{F}}$ stands for the unitary fast Fourier transform (FFT) matrix and $\mathbf{I}_m$ represents the $m \times m$ identity matrix.

II. System and data model

Consider a MIMO-OFDM system with N_t transmit and N_r receive antennas as depicted in Figure 1. At the transmitter, the input data stream is demultiplexed into N_t parallel substreams and each substream is mapped into frequency-domain quadrature phase-shift keying (QPSK) symbols and arranged into OFDM blocks of length N. Each block is then converted to the time domain by means of an N-point inverse fast Fourier transform (IFFT) and extended with a CP of length

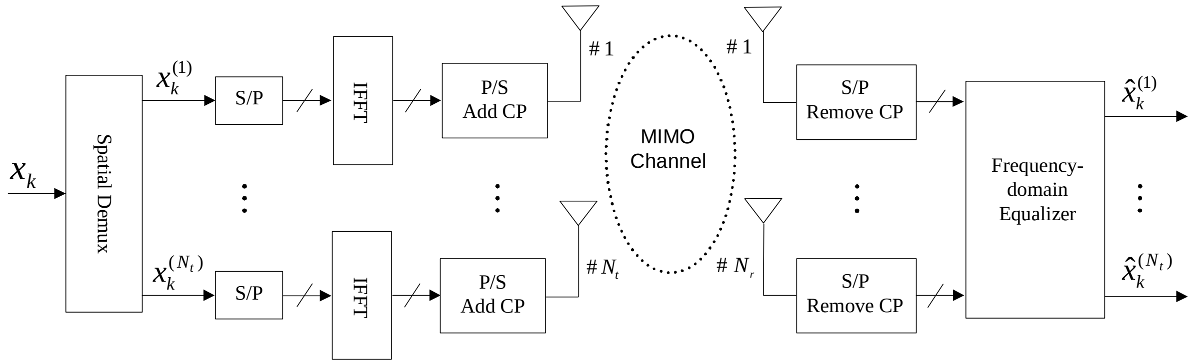

Fig. 1. MIMO-OFDM system model

c. The time-domain blocks of each substream are then serially transmitted over a doubly selective channel by one transmit antenna at a rate of $1/T$ symbols/s. At the receiver, after removing the CP, FFT demodulation as well as frequency-domain equalization are performed to detect the transmitted symbols. Let $x_k^{(t)}[i]$ represent the QPSK symbol transmitted on the kth subcarrier of the ith OFDM block in the tth substream. The time-domain sequence $u^{(t)}[n]$ transmitted from the tth antenna can then be written as

$$u^{(t)}[n] = \frac{1}{\sqrt{N}} \sum_{k=0}^{N-1} x_k^{(t)}[i] e^{j2\pi mk/N} \qquad (1)$$

where $i = \lfloor n/(N+c) \rfloor$ and $m = n - i(N+c) - c$.

We denote the impulse response of the channel characterizing the link between the tth transmit antenna and the rth receive antenna at time-index n and discrete time-delay θ as $g^{(r,t)}[n;\theta]$. Using the baseband-equivalent description, the received signal at the rth receive antenna at time-index n, $y^{(r)}[n]$ is given by

$$y^{(r)}[n] = \sum_{t=1}^{N_t} \sum_{\theta=0}^{+\infty} g^{(r,t)}[n;\theta] u^{(t)}[n-\theta] + \xi^{(r)}[n] \qquad (2)$$

where $\xi^{(r)}[n]$ is the additive noise which is assumed to be a zero-mean white complex Gaussian process that is independent of the transmitted sequence.

We use the complex exponential basis expansion model (CE-BEM) [8], [9] to describe the doubly selective channel $g^{(r,t)}[n;\theta]$ for $n \in \{\, i(N+c)+c+d-L'+1, \dots, (i+1)(N+c)+d \,\}$ where d is some synchronization (decision) delay and L' is a constant greater than or equal to the channel order L. In CE-BEM, the doubly selective channel $g^{(r,t)}[n;\theta]$ is approximated as a TV finite impulse response (FIR) filter $h^{(r,t)}[n;\theta]$ where each tap is modeled as a weighted sum of a few complex exponential basis functions. We express the lth tap of the TV FIR channel between the tth transmit antenna and the rth receive antenna at time-index n as

$$h^{(r,t)}[n;l] = \sum_{q=-Q/2}^{Q/2} h_{q,l}^{(r,t)} e^{j2\pi qn/K} \qquad (3)$$

where Q is the number of TV basis functions and K determines the CE-BEM frequency resolution, which is assumed to be larger than or equal to the number of subcarriers. The parameters Q and K should satisfy $Q/(2KT) \geq f_{max}$, where f_{max} is the channel maximum Doppler spread. Here, we assume that the CE-BEM frequency resolution K is an integer multiple of the FFT size i.e., $K = PN$, where P is an integer greater than or equal to 1. The CE-BEM coefficients $\left\{ h_{q,l}^{(r,t)} \right\}$ remain constant over a period of length $(N+L)T$ and may change from block to block.

Substituting (3) in (2), we can write the received sequence at the rth receive antenna as

$$y^{(r)}[n] = \sum_{t=1}^{N_t} \sum_{q=-Q/2}^{Q/2} \sum_{l=0}^{L} e^{j2\pi qn/K} h_{q,l}^{(r,t)} u^{(t)}[n-l] + \xi^{(r)}[n] \qquad (4)$$

We use matrix representation to express the received data block of length $N+L'$ at the rth receive antenna for $n \in \{i(N+c)+c+d-L'+1, \dots, (i+1)(N+c)+d\}$ as

$$\mathbf{y}^{(r)}[i] = \sum_{t=1}^{N_t} (\underbrace{\sum_{q=-Q/2}^{Q/2} \mathbf{\Omega}_q[i] \left[\mathbf{O}_1, \mathbf{H}_q^{(r,t)}[i], \mathbf{O}_2 \right] (\mathbf{I}_3 \otimes \mathbf{P})(\mathbf{I}_3 \otimes \boldsymbol{\mathcal{F}}^H)}_{\mathbf{G}^{(r,t)}[i]} \times \underbrace{\begin{bmatrix} \mathbf{x}^{(t)}[i-1] \\ \mathbf{x}^{(t)}[i] \\ \mathbf{x}^{(t)}[i+1] \end{bmatrix}}_{\tilde{\mathbf{x}}^{(t)}}) + \boldsymbol{\xi}^{(r)}[i] = \mathbf{G}^{(r)}[i]\tilde{\mathbf{x}} + \boldsymbol{\xi}^{(r)}[i] \qquad (5)$$

where i is the block index, $\mathbf{y}^{(r)}[i] = [y^{(r)}[i(N+c)+c+d-L'+1], \dots, y^{(r)}[(i+1)(N+c)+d]]^T$, $\mathbf{\Omega}_q[i] = \mathrm{diag}\{[e^{j2\pi q(i(N+c)+c+d-L'+1)/K}, \dots, e^{j2\pi q((i+1)(N+c)+d)/K}]\}$, $\mathbf{O}_1 = \mathbf{0}_{(N+L') \times (N+2c+d-L-L')}$, $\mathbf{O}_2 = \mathbf{0}_{(N+L') \times (N+c-d)}$, $\mathbf{H}_q^{(r,t)}[i]$ is an $(N+L') \times (N+L+L')$ Toeplitz matrix with the first column $[h_{q,L}^{(r,t)}[i]\,, \mathbf{0}_{1\times(N+L'-1)}]$ and the first row $[h_{q,L}^{(r,t)}[i]\,, \dots, h_{q,0}^{(r,t)}[i]\,, \mathbf{0}_{1\times(N+L'-1)}]$,

$\mathbf{x}^{(t)}[i] = [x_0^{(t)}[i], \ldots, x_{N-1}^{(t)}[i]]^T$, $\tilde{\mathbf{x}} = [\tilde{\mathbf{x}}^{(1)T}, \ldots, \tilde{\mathbf{x}}^{(N_t)T}]^T$, $\boldsymbol{\xi}^{(r)}[i] = [\xi^{(r)}[i(N+c)+c+d-L'+1], \ldots, \xi^{(r)}[(i+1)(N+c)+d]]^T$, $\mathbf{G}^{(r)}[i] = \left[\mathbf{G}^{(r,1)}[i], \ldots, \mathbf{G}^{(r,N_t)}[i]\right]$ and $\mathbf{P}$ is the CP insertion matrix given by

$$\mathbf{P} = \begin{bmatrix} \mathbf{0}_{c\times(N-c)} & \mathbf{I}_c \\ \mathbf{I}_N & \end{bmatrix}$$

Note that (5) is an extension of equation (22) in [10] to the MIMO-OFDM case. Defining $\mathbf{y}[i] = [\mathbf{y}^{(1)T}[i], \ldots, \mathbf{y}^{(N_r)T}[i]]^T$, $\mathbf{G}[i] = [\mathbf{G}^{(1)T}[i], \ldots, \mathbf{G}^{(N_r)T}[i]]^T$ and $\boldsymbol{\xi}[i] = [\boldsymbol{\xi}^{(1)T}[i], \ldots, \boldsymbol{\xi}^{(N_r)T}[i]]^T$, and using (5) we can write the received data blocks (each of length $N+L'$) at all receive antennas as

$$\mathbf{y}[i] = \mathbf{G}[i]\tilde{\mathbf{x}} + \boldsymbol{\xi}[i] \tag{6}$$

III. Per-tone equalization

In this section, we propose a per-tone frequency-domain interference cancellation and equalization technique to simultaneously mitigate ICI and IBI. In addition, our proposed equalization technique implicitly mitigates the co-antenna interference, which is the interference caused by the signals from multiple transmit antennas being received on the same receive antenna. We assume a general case, where the channel changes over an OFDM block and the channel delay span is greater than the CP. We derive our technique directly in the frequency domain.

In doubly selective fading, if the CP length is chosen to be larger than the channel delay span, IBI is completely eliminated and only ICI occurs due to channel time variations. It has been shown in [11] and [12] that ICI power on each subcarrier is originated from a few adjacent subcarriers. In other words, the desired subcarrier would be affected by only a few neighbors. Based on this fact, the QPSK symbol transmitted on the kth subcarrier of the ith OFDM block at the ath transmit antenna can be estimated using a linear combination of the frequency components corresponding to that subcarrier and its adjacent neighbors on different receive antennas. Considering Q' neighboring subcarriers, we express this linear combination as

$$\hat{x}_k^{(a)}[i] = \sum_{r=1}^{N_r} \sum_{q'=-Q'/2}^{Q'/2} \alpha_{q'}^{(r,a,k)}[i] y_{f,k+q'}^{(r)}[i] \tag{7}$$

where $y_{f,k+q'}^{(r)}[i]$ is the $(k+q')$th frequency component of the rth received signal, which is computed as $y_{f,k+q'}^{(r)}[i] = \boldsymbol{\mathcal{F}}^{(k+q')}[y^{(r)}[i(N+c)+c+d+1], \ldots, y^{(r)}[(i+1)(N+c)+d]]^T$ and $\boldsymbol{\mathcal{F}}^{(k+q')}$ is the $(k+q')$th row of the FFT matrix $\boldsymbol{\mathcal{F}}$. We can obtain the coefficients $\alpha_{q'}^{(r,a,k)}[i]$ using the mean-square error (MSE) criterion. However, in the case of insufficient CP and doubly selective fading, IBI is present in addition to ICI and the above simple linear combination is no longer a good estimate of $x_k^{(a)}[i]$. In other words, each frequency component in (7) includes some IBI power and hence, the linear combination of adjacent subcarriers will not lead to a proper estimate of the QPSK symbol transmitted on the kth subcarrier. To use (7) in the presence of both ICI and IBI, we implicitly remove the IBI power from the FFT output samples. To this end, we first perform $L'+1$ FFTs of size N on the $N+L'$ samples of each received signal. This is equivalent to performing a sliding FFT on each of the incoming signals. Then, we obtain the IBI-free frequency components through a linear combination of the sliding FFT outputs corresponding to each subcarrier.

We substitute the so-called IBI-free frequency components in (7) to extend it for joint ICI and IBI cancellation as follows:

$$\hat{x}_k^{(a)}[i] = \sum_{r=1}^{N_r} \sum_{q'=-Q'/2}^{Q'/2} \alpha_{q'}^{(r,a,k)}[i] (\boldsymbol{\beta}_{q'}^{(r,a,k)T}[i] \tilde{\boldsymbol{\mathcal{F}}}^{(k+q')} \mathbf{y}^{(r)}[i]) \tag{8}$$

where $\boldsymbol{\beta}_{q'}^{(r,a,k)}[i] = [\beta_{q',0}^{(r,a,k)}[i], \ldots, \beta_{q,L'}^{(r,a,k)}[i]]^T$ and

$$\tilde{\boldsymbol{\mathcal{F}}}^{(k+q')} = \begin{bmatrix} 0 & \cdots & 0 & \boldsymbol{\mathcal{F}}^{(k+q')} \\ \vdots & 0 & \boldsymbol{\mathcal{F}}^{(k+q')} & 0 \\ 0 & \iddots & 0 & \vdots \\ \boldsymbol{\mathcal{F}}^{(k+q')} & 0 & \cdots & 0 \end{bmatrix}$$

which represents a sliding FFT operation. Defining $\mathbf{w}_{q'}^{(r,a,k)T}[i] = \alpha_{q'}^{(r,a,k)}[i] \boldsymbol{\beta}_{q'}^{(r,a,k)T}[i]$ we can write (8) as

$$\hat{x}_k^{(a)}[i] = \sum_{r=1}^{N_r} \sum_{q'=-Q'/2}^{Q'/2} \mathbf{w}_{q'}^{(r,a,k)T}[i] \tilde{\boldsymbol{\mathcal{F}}}^{(k+q')} \mathbf{y}^{(r)}[i] \tag{9}$$

Equation (9) indicates that $\hat{x}_k^{(a)}[i]$ is estimated through a linear combination of the sliding FFT output samples on the kth subcarrier and its Q' neighbors. This combination can be viewed as a two-dimensional (time and frequency) interference cancellation scheme.

Using matrix representation, (9) reduces to

$$\hat{x}_k^{(a)}[i] = \mathbf{w}^{(a,k)H}[i] (\mathbf{I}_{N_r} \otimes \tilde{\mathbf{F}}^{(k)}) \mathbf{y}[i] \tag{10}$$

where $\mathbf{w}^{(a,k)}[i] = [\mathbf{w}^{(1,a,k)T}[i], \ldots, \mathbf{w}^{(N_r,a,k)T}[i]]^H$, $\mathbf{w}^{(r,a,k)}[i] = [\mathbf{w}_{-Q'/2}^{(r,a,k)T}[i], \ldots, \mathbf{w}_{Q'/2}^{(r,a,k)T}[i]]^T$, $\mathbf{w}_{q'}^{(r,a,k)}[i] = [w_{q',0}^{(r,a,k)}[i], \ldots, w_{q',L'}^{(r,a,k)}[i]]^T$ and $\tilde{\mathbf{F}}^{(k)} = [\tilde{\boldsymbol{\mathcal{F}}}^{(k-Q'/2)T}, \ldots, \tilde{\boldsymbol{\mathcal{F}}}^{(k+Q'/2)T}]^T$.

From (10), we can see that each subcarrier corresponding to each transmit substream or each transmit antenna, has its own equalizer $\mathbf{w}^{(a,k)}[i]$ and thus, the equalizer coefficients can be optimized for each subcarrier (tone) separately. To obtain the per-tone equalizer (PTEQ) $\mathbf{w}^{(a,k)}[i]$ for the kth subcarrier of the ath transmit antenna, we define the following MSE cost function

$$\mathcal{J}[i] = \mathcal{E}\left\{ \left| x_k^{(a)}[i] - \mathbf{w}^{(a,k)H}[i] (\mathbf{I}_{N_r} \otimes \tilde{\mathbf{F}}^{(k)}) \mathbf{y}[i] \right|^2 \right\} \tag{11}$$

Hence, the minimum MSE (MMSE) coefficients for the kth subcarrier are obtained by solving $\partial\mathcal{J}[i]/\partial\mathbf{w}^{(a,k)}[i]=0$ which reduces to

$$\mathbf{w}^{(a,k)}_{\mathrm{MMSE}}[i]= \Big((\mathbf{I}_{N_r}\otimes\tilde{\mathbf{F}}^{(k)})(\mathbf{G}[i]\mathbf{R}_{\tilde{\mathbf{x}}}\mathbf{G}^H[i]+\mathbf{R}_{\xi})(\mathbf{I}_{N_r}\otimes\tilde{\mathbf{F}}^{(k)H})\Big)^{-1} \times(\mathbf{I}_{N_r}\otimes\tilde{\mathbf{F}}^{(k)})\mathbf{G}[i]\mathbf{R}_{\tilde{\mathbf{x}}}\mathbf{e}^{(k)} \quad (12)$$

where $\mathbf{R}_{\tilde{\mathbf{x}}}=\mathcal{E}\{\tilde{\mathbf{x}}\tilde{\mathbf{x}}^H\}=\sigma_s^2\mathbf{I}_{(3N_tN)}$, $\mathbf{R}_{\xi}=\sigma_{\xi}^2\mathbf{I}_{N_r(N+L')}$, σ_s^2 and σ_{ξ}^2 are the QPSK symbol power and the noise variance, respectively and $\mathbf{e}^{(k)}$ is the $(3N_tN)\times1$ unit vector with a 1 in the position $3N(a-1)+N+k$. Figure 2 illustrates the proposed per-tone equalizer for the kth subcarrier of the ath transmit antenna. As shown in this figure, one sliding FFT is needed per receive antenna to compute (10).

IV. Complexity reduction

In section 3, we showed that to estimate the transmitted symbol on each subcarrier, the proposed PTEQ requires N_r sliding FFTs. In this section, we use a procedure similar to that of [13] to reduce the complexity of the proposed PTEQ. This procedure replaces each sliding FFT with one full FFT and the remaining FFTs are compensated for by L' difference terms based on the following property:

$$\tilde{\boldsymbol{\mathcal{F}}}^{(k+q')}\mathbf{y}^{(r)}[i]=\mathbf{T}^{(k+q')}\begin{bmatrix} y^{(r)}_{f,\,k+q'}[i]\\ \Delta\mathbf{y}^{(r)}[i]\end{bmatrix} \quad (13)$$

where $y^{(r)}_{f,\,k+q'}[i]$ is the FFT output sample on the $(k+q')$th subcarrier at the rth receive antenna, $\mathbf{T}^{(k+q')}$ is an $(L'+1)\times(L'+1)$ lower triangular Toepolitz matrix given by

$$\mathbf{T}^{(k+q')}=\begin{bmatrix} 1 & 0 & \cdots & 0\\ \vartheta^{(k+q')} & \ddots & \ddots & \vdots\\ \vdots & \ddots & \ddots & 0\\ \vartheta^{(k+q')L'} & \cdots & \vartheta^{(k+q')} & 1\end{bmatrix}$$

with $\vartheta=e^{-j2\pi/N}$, and the difference terms $\Delta\mathbf{y}^{(r)}[i]$ are $\Delta\mathbf{y}^{(r)}[i]=[y^{(r)}[i(N+c)+c+d]-y^{(r)}[(i+1)(N+c)+d],\ldots,y^{(r)}[i(N+c)+c+d-L'+1]-y^{(r)}[(i+1)(N+c)+d-L'+1]]^T$.

We substitute (13) in (9) to obtain

$$\hat{x}^{(a)}_k[i]=\sum_{r=1}^{N_r}\sum_{q'=-Q'/2}^{Q'/2}\mathbf{w}^{(r,a,k)T}_{q'}[i]\mathbf{T}^{(k+q')}\begin{bmatrix} y^{(r)}_{f,\,k+q'}[i]\\ \Delta\mathbf{y}^{(r)}[i]\end{bmatrix} \quad (14)$$

Introducing $\boldsymbol{\upsilon}^{(r,a,k)T}_{q'}[i]=\mathbf{w}^{(r,a,k)T}_{q'}[i]\mathbf{T}^{(k+q')}$, $\boldsymbol{\gamma}^{(r,a,k)}_1[i]=[\upsilon^{(r,a,k)}_{-Q'/2,0}[i],\ldots,\upsilon^{(r,a,k)}_{Q'/2,0}[i]]^T$ and $\boldsymbol{\gamma}^{(r,a,k)}_2[i]=\left[\sum_{q'=-Q'/2}^{Q'/2}\upsilon^{(r,a,k)}_{q',1}[i],\ \ldots,\ \sum_{q'=-Q'/2}^{Q'/2}\upsilon^{(r,a,k)}_{q',L'}[i]\right]^T$

we rewrite (14) as follows

$$\hat{x}^{(a)}_k[i]=\sum_{r=1}^{N_r}[\boldsymbol{\gamma}^{(r,a,k)T}_1[i],\boldsymbol{\gamma}^{(r,a,k)T}_2[i]]\times\begin{bmatrix} y^{(r)}_{f,\,k-Q'/2}[i]\\ \vdots\\ y^{(r)}_{f,\,k+Q'/2}[i]\\ \Delta\mathbf{y}^{(r)}[i]\end{bmatrix} =\sum_{r=1}^{N_r}\mathbf{v}^{(r,a,k)T}[i]\times\underbrace{\begin{bmatrix} \mathbf{0}_{1\times L'} & \boldsymbol{\mathcal{F}}^{(k-Q'/2)} & \\ \vdots & \vdots & \\ \mathbf{0}_{1\times L'} & \boldsymbol{\mathcal{F}}^{(k+Q'/2)} & \\ \bar{\mathbf{I}}_{L'} & \mathbf{0}_{L'\times(N-L')} & -\bar{\mathbf{I}}_{L'}\end{bmatrix}}_{\hat{\mathbf{F}}^{(k)}}\mathbf{y}^{(r)}[i] \quad (15)$$

where $\mathbf{v}^{(r,a,k)}[i]=[\boldsymbol{\gamma}^{(r,a,k)T}_1[i],\boldsymbol{\gamma}^{(r,a,k)T}_2[i]]^T$ and $\bar{\mathbf{I}}_{L'}$ is the anti-diagonal identity matrix of size $L'\times L'$. Defining $\mathbf{v}^{(a,k)}[i]=[\mathbf{v}^{(1,a,k)T}[i],\ldots,\mathbf{v}^{(N_r,a,k)T}[i]]^H$, (15) can finally be written as

$$\hat{x}^{(a)}_k[i]=\mathbf{v}^{(a,k)H}[i](\mathbf{I}_{N_r}\otimes\hat{\mathbf{F}}^{(k)})\mathbf{y}[i] \quad (16)$$

Similar to (11), we can obtain the MMSE PTEQ $\mathbf{v}^{(a,k)}[i]$ for the kth subcarrier on the ath transmit antenna by minimizing the following cost function

$$\mathcal{J}[i]=\mathcal{E}\left\{\left|x^{(a)}_k[i]-\mathbf{v}^{(a,k)H}[i]\left(\mathbf{I}_{N_r}\otimes\hat{\mathbf{F}}^{(k)}\right)\mathbf{y}[i]\right|^2\right\} \quad (17)$$

Figure 3 shows the derived low-complexity PTEQ scheme for the kth subcarrier of the ath transmit antenna.

V. Unifying framework

In this section, we illustrate that our proposed per-tone equalizer unifies and extends several previously proposed frequency-domain equalization approaches as follows.

(i) SISO-OFDM over frequency selective channels $(Q=0)$

- $c\geq L$ and $L'=0$: the proposed PTEQ reduces to the one-tap frequency-domain equalizer (FEQ) as in [14];
- $c<L$ and $L'\neq0$: the proposed PTEQ reduces to the per-tone equalizer proposed for discrete multi-tone transmission (DMT)-based systems in [15].

(ii) SISO-OFDM over doubly selective channels $(Q\neq0)$

- $c\geq L$, $L'=0$, and $P=1$: the proposed PTEQ boils down to the FEQs proposed in [12] and [16]; and corresponds to the PTEQ proposed in [17].

(iii) SIMO-OFDM over doubly selective channels $(Q\neq0)$

- $c<L$, $L'\neq0$, and $P=1$: the proposed PTEQ reduces to the FEQ proposed in [10];
- $c<L$, $L'\neq0$ and $P\geq1$: the proposed PTEQ reduces to the FEQ proposed in [18].

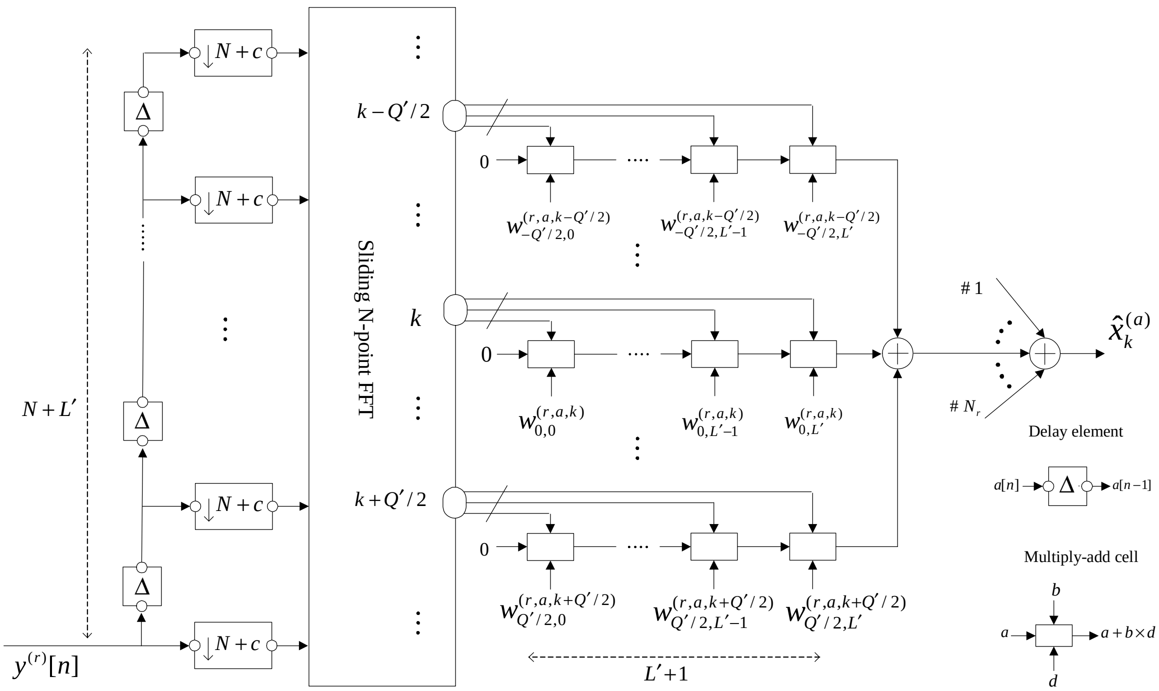

Fig. 2. Proposed per-tone equalizer (PTEQ) for the kth subcarrier of the ath transmit antenna

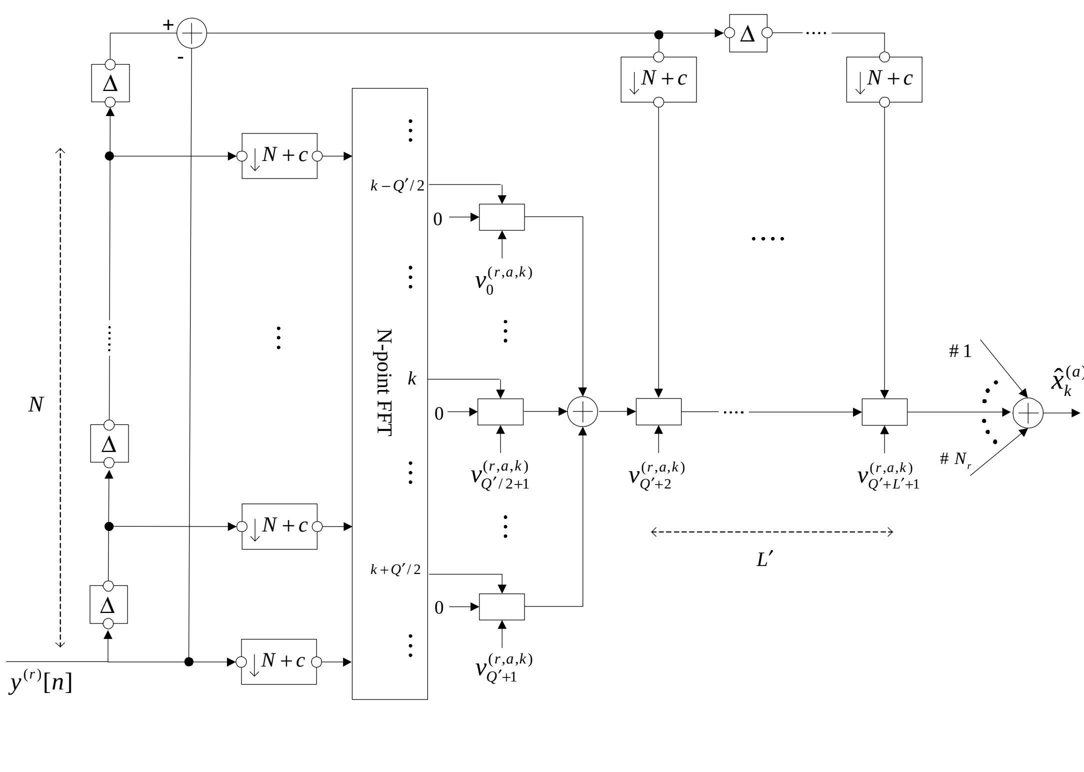

Fig. 3. Low-complexity scheme of the proposed PTEQ for the kth subcarrier of the ath transmit antenna

VI. Simulation results

We now demonstrate the performance of the proposed equalizer through computer simulations. We consider a MIMO-OFDM system with $N_t = 2$ transmit antennas and $N_r = 4$ receive antennas. The doubly selective channel is of order $L = 6$ with a maximum Doppler spread of $f_{max} = 100Hz$. The channel taps are generated as independent identically distributed (i.i.d.) random variables and correlated in time with a correlation function according to Jakes' model $\mathcal{E}\{h^{(r_1,t_1)}[n_1;l_1]h^{(r_2,t_2)*}[n_2;l_2]\} = \sigma_h^2 J_0(2\pi f_{\max} T(n_1 - n_2))\delta[l_1 - l_2]\delta[r_1 - r_2]\delta[t_1 - t_2]$, where J_0 is the zero-order Bessel function of the first kind and σ_h^2 represents the variance of the channel gain. The number of subcarriers in each OFDM block is $N = 128$, the CP length is $c = 3$ and the sampling time is $T = 50\,\mu sec$.

We approximate the simulated channel using the CE-BEM. The CE-BEM resolution is determined by $K = PN$ where P is chosen as $P = 1, 2$ and the number of complex exponentials is $Q = 4$. We consider $L' = 8, Q' = 8$ and the delay $d = 3$. We use both the proposed PTEQ and the one-tap MMSE FEQ to equalize the true (simulated) Jakes' channel. The one-tap equalizer used here is an extension of the one-tap FEQ in [14] for SISO-OFDM. The difference between this equalizer and the conventional one-tap equalizer is that it is designed by minimizing the MSE cost function at the equalizer output.

Figure 4 illustrates the simulation results for bit-error-rate (BER) vs. signal-to-noise ratio (SNR). We define the SNR as $\text{SNR} = \sigma_h^2(L+1)\sigma_s^2/\sigma_\xi^2$. As shown in this figure, the one-tap MMSE FEQ cannot mitigate the interference well. For CE-BEM resolution $P = 1$, the proposed PTEQ considerably outperforms the one-tap equalizer, however, it suffers from an early error floor at BER = 2.8×10^{-3} and SNR = 18 dB. We also see in this figure that the performance of the proposed method is significantly improved when $P = 2$.

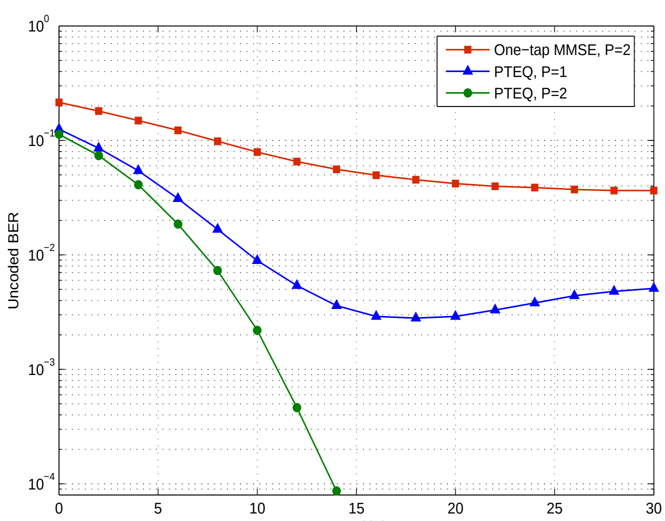

Fig. 4. BER vs. SNR for MIMO-OFDM with $N_t = 2$ and $N_r = 4$

VII. Conclusion

We proposed a per-tone equalization approach for MIMO-OFDM over doubly selective channels, when an insufficient CP is used. The proposed equalizer is directly designed in the frequency domain and can be viewed as a two-dimensional (time and frequency) interference cancellation scheme. Moreover, it unifies many existing equalization approaches. Simulation results show that increasing the CE-BEM frequency resolution to twice that of the FFT, leads to significant performance improvement.

References

[1] Q. Li, X. E. Lin, J. Zhang, and W. Roh, "Advancement of MIMO technology in WiMAX: from IEEE 802.16d/e/j to 802.16m," *IEEE Commun. Mag.*, vol. 47, no. 6, pp. 100-107, June 2009.

[2] T. Hwang, Ch. Yang, G. Wu, Sh. Li, and G. Ye Li, "OFDM and its wireless applications: a survey," *IEEE Trans. Veh. Technol.* vol. 58, no. 4, pp. 1673-1694, May 2009.

[3] A. Stamoulis, S. N. Diggavi, and N. Al-Dhahir, "Intercarrier interference in MIMO OFDM," *IEEE Trans. Signal Process.*, vol. 50, no. 10, pp. 2451-2464, Oct. 2002.

[4] R. Chen, Y. Xu, H. Zhang, and H. Luo, "Iterative ICI mitigation method for MIMO OFDM systems," *IEICE Trans. Commun.*, vol. E89-B, no. 3, pp. 859-866, March 2006.

[5] V.-D. Nguyen, M. Patzold, F. Maehara, H. Haas, and M.-V. Pham, "Channel estimation and interference cancellation for MIMO-OFDM," *IEICE Trans. Commun.*, vol. E90-B, no. 2, pp. 277-290, Feb. 2007,.

[6] Sh. Ma and T.-S. Ng, "Two-step signal detection for MIMO-OFDM systems without cyclic prefix," in *Proc. IEEE Wireless Commun. and Net., WCNC*, April 2009, pp. 1-6.

[7] C.-Y. Hsu and W.-R. Wu, "Low-complexity ICI mitigation methods for high-mobility SISO/MIMO-OFDM systems," *IEEE Trans. Veh. Technol.*, vol. 58, no. 6, pp. 2755-2768, July 2009.

[8] G. B. Giannakis and C. Tepedelenlioğlu, "Basis expansion models and diversity techniques for blind identification and equalization of time varying channels," *Proc. IEEE*, vol. 86, no. 10, pp. 1969-1986, Oct. 1998.

[9] G. Leus, S. Zhou, and G. B. Giannakis, "Orthogonal multiple access over time- and frequency-selective fading," *IEEE Trans. Inf. Theory*, vol. 49, no. 8, pp. 1942-1950, Aug. 2003.

[10] I. Barhumi, G. Leus, and M. Moonen, "Equalization for OFDM over doubly selective channels," *IEEE Trans. Signal Process.*, vol. 54, no. 4, pp. 1445-1458, April 2006.

[11] P. Robertson and S. Kaiser, "The effects of Doppler spreads in OFDM(A) mobile radio systems," in *Proc. IEEE Veh. Technol. conf.*, Sep. 19-22, 1999, vol. 1, pp. 329-333.

[12] X. D. Cai, and G. B. Giannakis, "Bounding performance and suppressing intercarrier interfenence in wireless mobile OFDM," *IEEE Trans. Commun.*, vol. 51, no. 12, pp. 2047-2056, Dec. 2003.

[13] B. Farhang-Boroujeny and S. Gazor, "Generalized sliding FFT and its application to implementation of block LMS adaptive filters," *IEEE Trans. Signal Process.*, vol. 42, no. 3, pp. 532-538, Mar. 1994.

[14] Z. Wang and G. B. Giannakis, "Wireless multicarrier communications: where Fourier meets Shannon," *IEEE Signal Process. Mag.*, vol. 17, no. 3, pp. 29-48, May 2000.

[15] K. Van Acker, G. Leus, M. Moonen, O. Van deWiel, and T. Pollet, "Per-tone equalization for DMT-based systems," *IEEE Trans. Commun.*, vol. 49, no. 1, pp. 109-119, Jan. 2001.

[16] X. Huang and H.-C. Wu, "Robust and efficient intercarrier interference mitigation for OFDM systems in time-varying fading channels," *IEEE Trans. Veh. Technol.*, vol. 56, no. 5, pp. 2517-1528, Sep. 2007.

[17] I. Barhumi, G. Leus, and M. Moonen, "Frequency-domain equalization for OFDM over doubly selective channels," in *Proc. 6th Baiona Workshop Signal Process. Commun.*, Sep. 2003, pp. 103-107.

[18] M. Beheshti, M. J. Omidi, and A. M. Doost-Hoseini, "Equalization of SIMO-OFDM systems with insufficient cyclic prefix in doubly selective channels," *IET Commun.*, vol. 3, no. 12, pp. 1870-1882, Dec. 2009.